ELSEVIER

Contents lists available at ScienceDirect

Physica B: Condensed Matter

journal homepage: www.elsevier.com/locate/physb





Effect of heat treatment and gamma irradiation on TL emission sensitivity of blue quartz crystal

Betzabel N. Silva-Carrera ^a, Nilo F. Cano ^{b,*}, Felix V.S. Cruz ^c, Edwin J. Pilco ^d, T.K. Gundu Rao ^d, J.F. Benavente ^e, José F.D. Chubaci ^{a,c}

- ^a Instituto de Pesquisas Energéticas e Nucleares, IPEN-CNEN/SP, São Paulo, SP, Brazil
- b Universidade Federal de São Paulo, Instituto do Mar. SP. Brazil
- Universidade de São Paulo, Instituto de Física, São Paulo, SP, Brazil
- ^d Universidad Nacional de San Agustín de Arequipa UNSA, Arequipa, Peru
- e CIEMAT, Av. Complutense 40 E, 28040, Madrid, Spain

ARTICLE INFO

Keywords: Blue quartz TL emission spectrum Sensitization Dosimetry Effect of heat treatment and gamma irradiation

ABSTRACT

The combined effect of heat treatment and irradiation on the thermoluminescent response of natural blue quartz was studied. Samples were subjected to different heat treatment temperatures, pre-dose doses, and thermal activation temperatures to sensitize the Thermoluminescence (TL) response of blue quartz. Blue quartz pellets produced by sintering at 1200 $^{\circ}$ C were sensitized with a combination of different pre-doses and thermal activation temperatures. It was found that the maximum TL intensity occurred for a pre-dose of 500 Gy and a thermal activation temperature of 550 $^{\circ}$ C, resulting in a dosimetric peak with a TL signal 150 times more intense than the initial one. The kinetic parameters of the TL glow curve of the sensitized pellets were analyzed by the methods of different heating rates, Tm-Tstop, and deconvolution. The dosimetric properties of the sensitized blue quartz pellets were also evaluated using the 220 $^{\circ}$ C TL peak.

1. Introduction

There is a wide variety of quartz colors in nature, depending on the inclusions, atomic arrangement, impurities, and defects present in its crystal structure. If quartz is pure, it is colorless (transparent and crystalline) and very rigid. The main-colored varieties of quartz include citrine (yellow), amethyst (violet), smoky quartz (grey-brown), rose quartz, green quartz, and blue quartz, among others.

The use of quartz as a Thermoluminescence (TL) material has been widely explored in areas such as geological [1,2] and archaeological dating [3,4], and in retrospective dosimetry [5], where it is determined when sediment grains from Quaternary deposits were last exposed to daylight. The sediments that are suitable for luminescence dating range from aeolian to coastal, fluvial, periglacial, and glacial [6].

The TL glow curve of alpha quartz is well documented. Franklin et al. [7] identified TL peaks at 100, 180, 220, 260, 305, 350, and 450 $^{\circ}$ C in sedimentary quartz from Australia and determined that the TL peaks at 260, 350, and 450 $^{\circ}$ C emit light at 470 nm, while the other smaller peaks appear to emit light at 435 nm.

Farias et al. [8] studied the thermoluminescent behavior of seven

varieties of natural quartz from Brazil subjected to heat treatment at 600 $^{\circ}\text{C}$ and irradiated with a dose of 10 kGy from a ^{60}Co source. These authors observed that blue quartz presented TL glow peaks with good intensity centered at 220 $^{\circ}\text{C}$ and 350 $^{\circ}\text{C}$. Recently, Márquez-Mata et al. [9] investigated the thermoluminescent characteristics of seven quartz varieties from Mexico and compared their TL response with commercial TLD-100 dosimeters. Of all the varieties, amethyst presented the best TL response, with peaks at 130, 202, and 287 $^{\circ}\text{C}$.

Zimmerman [10] explained the sensitization of the TL response of quartz by a phenomenological model involving an increased probability of radiative recombination at luminescent sites or centers. Sensitization was produced by heat treatments and irradiation doses (pre-dose effect) and allowed her to demonstrate, by this model, that sensitization decreases the supralinearity for the TL peak at 110 $^{\circ}$ C of quartz; she thereby proposed the trap competition model.

The TL emission spectrum of quartz generally comprises three main bands centered at: 380 nm (3.3 eV), 470 nm (2.6 eV) and 620 nm (2.0 eV). Other emissions have also been described, in the region of 420–435 nm for igneous quartz and 560–580 nm for hydrothermal vein quartz [11–13].

E-mail addresses: nilocano@if.usp.br, nilo.cano@unifesp.br (N.F. Cano).

^{*} Corresponding author.

Khoury et al. [14] studied the effect of radiation on sensitization TL peaks at 110 and 300 $^{\circ}$ C in natural quartz from different locations in Brazil. The TL glow curves of the samples before sensitization showed a well-defined TL peak at 110 $^{\circ}$ C, whereas, in the case of samples sensitized with a dose of 25 kGy, the TL glow curve showed two peaks centered at 85 and 298 $^{\circ}$ C. With these results, they concluded that it is possible to sensitize high-temperature TL peaks with gamma radiation and that the sensitization will depend on the origin of the quartz. According to Guzzo et al. [15], the centers acting as electron traps responsible for the TL peak around 300 $^{\circ}$ C are associated with Li impurities, and increasing ratios of Li to Al (Li/Al) and Li to OH (Li/OH) concentrations are favorable conditions for TL emission in the region between 200 and 400 $^{\circ}$ C.

Nascimento et al. [16] studied natural quartz from the municipality of Solonópole for use in radiodiagnostics. Previously, they sensitized the samples with heat treatment at 500 °C for 2 h and subjected them to a gamma radiation dose of 25 kGy from the ^{60}Co source. From his results, they conclude that Solonopole quartz had properties suitable for use as a dosimeter

Junior et al. [17] produced Solonopole quartz pellets using Teflon as a binder in a 1:1 ratio of mass under a pressure of 5 kN and subjected them to a heat treatment at 400 $^{\circ}\text{C}$ for 20 h. They then sensitized the pellets with a dose of 25 kGy from a ^{60}Co source. The TL glow curve of the sensitized sample showed TL peaks around 110 and 310 $^{\circ}\text{C}$ for a test dose of 50 mGy.

Recently, Cunha et al. [18] studied the thermoluminescent response of quartz pellets produced by Teflon binding at a 1:1 mass ratio. When irradiated with an X-ray beam for mammography, the TL peak studied was 299 $^{\circ}$ C, with doses between 3.24 and 20.60 mGy, and the TL glow curve showed linearity, reproducibility, and good sensitivity for their application.

As we can see, there are studies on the TL glow curves of some varieties of quartz sensitized by a combination of high irradiation doses and thermal treatments, which show promise for application in radiation dosimetry. However, most studies using quartz as a dosimeter have employed some type of binder (such as Teflon). Teflon is a polymer that, after several heat treatments, loses its binding properties, resulting in a loss of mechanical stiffness of the dosimeter. In addition, there are no studies on the TL properties of blue quartz with possible applications in radiation dosimetry. Therefore, in this work, a systematic study of the TL properties of blue quartz sensitized by heat treatment and irradiation has been carried out. In addition, the dosimetric properties of blue quartz pellets produced by mechanical compaction and sintering at high temperature, i.e., without using a binder, have been investigated.

2. Material and methods

2.1. Material preparation

The natural blue quartz sample used in this study was purchased from the LEGEP stone store in São Paulo, Brazil. Fig. 1 shows a picture of the natural blue quartz with white spots, possibly due to the presence of colorless quartz. The blue quartz sample was crushed and sieved to retain grains of 0.018 and 0.080 mm in size for powder TL studies, while grains smaller than 0.018 mm in diameter were used in structural and compositional analysis by X-ray diffraction (XRD) and X-ray fluorescence (XRF), respectively.

To study the combined effect of heat treatments and irradiations on the sensitization of their TL response and to investigate their dosimetric properties of natural blue quartz, pellets of 6 mm diameter, 1 mm thickness, and 50 mg mass were produced by pressing the fine powdered material in a circular stainless-steel mold at 1.5 mega pounds for 25 s and sintering them at a temperature of 1200 $^{\circ}\mathrm{C}$ for 1 h in a single-air atmosphere. Fig. 1 shows the whole process of obtaining pellets: the stainless-steel mold and the blue quartz pellets produced.



Fig. 1. (Top) Sample of the blue quartz crystal, as received and in powder form, was used to produce the pellets. (Bottom) Stainless steel mold used to press the sample and images of the blue quartz pellets sintered at high temperatures. (For interpretation of the references to color in this figure legend, the reader is referred to the Web version of this article.)

2.2. Characterization technique

The morphological analysis of the quartz grains before and after the sensitization process was performed using a Jeol model JSM-IT700HR scanning electron microscope (SEM) coupled to energy dispersive spectroscopy (EDS), which allows qualitative determination of the distribution and homogeneity of the constituent elements of the sample.

A Rigaku Miniflex X-ray diffractometer, model 600, equipped with $\text{CuK}\alpha$ radiation, was used to evaluate the crystal structure of natural blue quartz and those heat-treated and sensitized. X-ray diffraction (XRD) data were recorded in the range of $15^\circ \leq 2\theta \leq 70^\circ$, with steps of $0.02^\circ.$ The XRD patterns were compared with the diffraction patterns of the quartz crystal using the QualX program.

TL measurements were performed with a Harshaw TL reader, model 4500, equipped with an EMI 9235QB photomultiplier tube (PMT), through a combination of the BG3 and BG39 filters (overall transmission band from 350 to 450 nm). TL measurements were performed in a flow of inert nitrogen gas up to a heating temperature of 400 $^{\circ}\text{C}$ with a heating rate of 2 $^{\circ}\text{C/s}$. Except for TL measurements at different heating rates. Five TL reading measurements were performed to obtain an average TL glow curve. TL emission spectrum measurements were carried out using a Risø TL/OSL reader by connecting a monochromator in front of the TL light detection system.

Three sources were used for sample irradiations: (1) a Philips MG 225/450 industrial X-ray unit, (2) a ^{137}Cs gamma source with a dose rate of 9.44 $\mu\text{Gy/s}$, and (3) a ^{60}Co gamma source of the Gamma-Cell type with a dose rate of 281.47 Gy/h. During irradiation, the pellets were placed on red polymethylmethacrylate (PMMA) supports (see Fig. 1). The irradiations were performed at room temperature and under electronic equilibrium conditions.

2.3. Numerical methods

2.3.1. Computer glow curve deconvolution (CGCD)

The experimental TL glow curves were analyzed using deconvolution methods based on a combination of linear functions associated with the first-order kinetics (FOK) model. Initially, parameters such as n(E) (density of trapped electrons in cm $^{-3}$), s (frequency factor in s $^{-1}$), material temperature (T in $^{\circ}$ C), heating rate (β in $^{\circ}$ C/s), and distribution width (σ in eV) were considered as independent variables, as described

by the following expression:

$$I(T_{i}) = \sum_{i=1}^{n} {}^{i}F(n_{o}, {}^{i}s, {}^{i}E, \sigma_{i}; T_{i})$$
(1)

The analytical expression ${}^{\rm i}{\rm F}$ for approximations based on the FOK model can be expressed as:

$$F = \frac{s}{\beta} \cdot \int_{0}^{+\infty} n(E) \cdot e^{-E/KT} \cdot \exp\left(-\frac{s}{\beta} \int_{T_0}^{T} e^{-E/KT} \cdot dT\right) \cdot dE$$
 (2)

where n(E) are functions that describe the density of trapped charges associated with the energy E. In the case of continuous trap distribution, this function can be written by a Gaussian expression [19]:

$$n(E) = \frac{n_0}{\sqrt{2 \cdot \pi \cdot \sigma^2}} e^{-(E - E_0)/2\sigma^2} \tag{3}$$

or localized electron trap distributions ($\sigma = 0.0$):

$$n(E) = n_0 \times \delta(E - E_0) \tag{4}$$

The set of parameters (n, β, s) does not establish a direct relationship between the geometric shape of the TL glow curve and the intrinsic parameters of the TL system. Therefore, by applying a maximum condition [19] as follows:

$$\frac{\mathrm{d}[\ln(\mathrm{I})]}{\mathrm{d}\mathrm{T}}\Big|_{\mathrm{T-Tm}} = 0 \tag{5}$$

Obtaining the following expression:

$$\frac{E}{K_b \cdot T_m^2} = \frac{S}{\beta} \times exp\left(-\frac{E}{K_b \cdot Tm}\right) \tag{6}$$

This approach enables the rewriting of equation (4) in terms of geometric parameters (E, I_{Max} , Tm), which correspond to the kinetic parameters of the system.

2.3.2. Tm-Tstop method

The Tm-Tstop method [20] consists in heating the sample to a specific temperature, Tstop, to thermally clean it, followed by recording its TL curve. The position of the first TL peak (Tm) corresponding to each Tstop is then identified and the stopping temperature is plotted against the temperature of the first maximum. This method allows to determine both the number of components present and to differentiate between regions with continuous electron trap distributions (where the Tm-Tstop pattern exhibits an increasing slope) and localized trap distributions, characterized by a slope close to zero.

2.3.3. Vary-heating-rates method

The activation energy value can be determined by taking the natural logarithm of expression (6) and analyzing the slope of the linear plot of $Ln\left(T_{m/\beta}^{2}\right)$ versus a $^{1}/_{K_{b}}$ Tm. This method is highly sensitive to the position of the peak temperature (Tm), and factors such as thermal lag may influence the linearity of the approach. Additionally, thermal quenching can cause shifts in the linear trend [21], leading to variations in the activation energy values obtained through this method.

3. Results and discussion

3.1. Structural and chemical composition analysis

The chemical composition of natural blue quartz was determined by X-ray fluorescence (XRF) analysis. The results of this analysis are presented in Table 1. As a result of the chemical analysis, the main components were found to be ${\rm SiO_2}$, ${\rm Al_2O_3}$, and ${\rm K_2O}$ with mean amounts of 77.4 %, 4.0 %, and 3.09 %, respectively. In addition, an appreciable content of ${\rm Fe_2O_3}$ (0.45 %) and ${\rm TiO_2}$ (0.292 %) is observed. Other oxides, such as ${\rm P_2O_5}$, CaO, ZrO₂, and As₂O₃, have also been detected. These impurities may play an important role in the TL properties of blue quartz.

Fig. 2 presents the SEM images of the blue quartz samples before (Fig. 2(a)) and after (Fig. 2(b)) the sensitization process. This result shows that the surfaces of both quartz samples are homogeneous and similar, indicating that the heat treatment and irradiation (in the sensitization process) do not alter the morphology of the blue quartz particles. Elemental mapping profiles (Fig. 2(c) to 2(g)) and EDS spectra (Fig. 2(h)) of one of the quartz particles confirm the uniform presence of

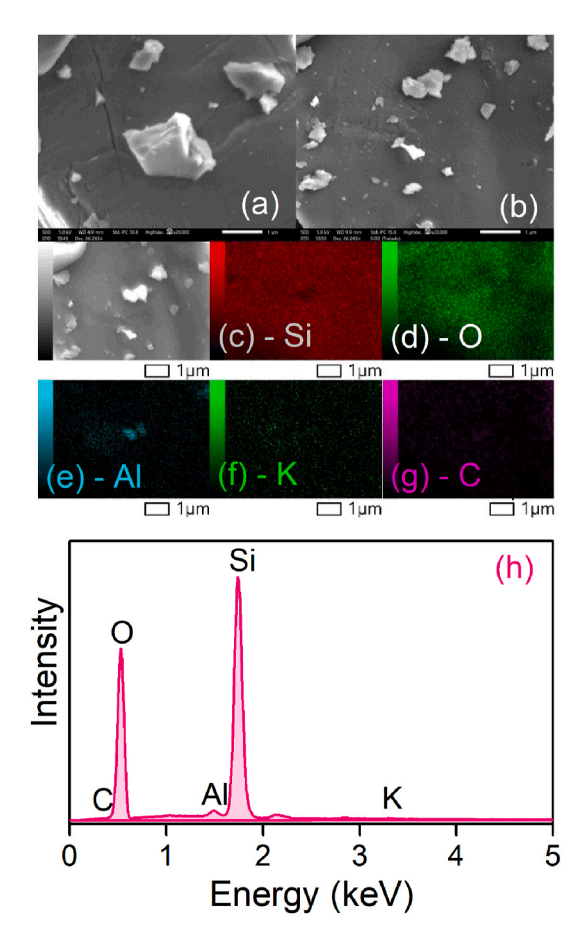


Fig. 2. (a) and (b) SEM images at 20000 times magnification of blue quartz grains before and after the sensitization process, respectively. (c–g) elemental mapping and (h) EDS analysis for a blue quartz particle. (For interpretation of the references to color in this figure legend, the reader is referred to the Web version of this article.)

Table 1
Main blue quartz components (wt%) determined by XRF analysis.

Sample		Compound (wt%)									
Blue quartz	SiO ₂ 77.4	Al ₂ O ₃ 4.00	K ₂ O 3.09	SO ₃ 0.84	Fe ₂ O ₃ 0.45	TiO_2 0.292	P ₂ O ₅ 0.084	CaO 0.035	ZrO_2 0.032	SrO 0.019	As ₂ O ₃ 0.006

Si, O, Al, and K in the quartz sample. These results are in agreement with the XRF results. It is worth mentioning that the presence of C (Fig. 2(g)) in the EDS analysis is due to the use of carbon tape in the experimental setup for electrical conduction.

Fig. 3 shows the X-ray diffraction (XRD) patterns of the blue quartz sample as received, after heat treatment at 1200 $^{\circ}$ C, and of the blue quartz pellet after the sensitization process with pre-dosing and activation heat treatment. The diffractograms present the main diffraction peaks of quartz with trigonal structure (SiO₂, JCPDS 05–0492). There were no significant changes in the intensity and position of the XRD peaks.

3.2. TL analysis

The sensitization of its TL response of powdered blue quartz was carried out by two methods: (i) heat treatment on the as-received sample and (ii) the pre-dose method on the previously heat-treated sample [22], followed by the effect of thermal activation temperature, which consists of heat treatment after preliminary irradiation.

Preliminary studies on the effect of heat treatment on powdered blue quartz showed a higher TL intensity for heat treatment of $1200\,^{\circ}\mathrm{C}$ for 1 h. From this result, this temperature was established as the sintering temperature for the production of blue quartz pellets. Moreover, with this sintering temperature, it was possible to obtain pellets with good mechanical strength for transport and handling.

A total of 140 blue quartz pellets were produced and separated into groups of 20 pellets to assess the sensibilization of their TL response with different gamma irradiation pre-doses [23] of 50, 500 Gy, 1, 2, 5, 10, and 20 kGy. After irradiation with the above radiation doses, the pellets were heat treated at 400 °C for 1 h to remove any induced TL signal and then irradiated with a test dose of 1 Gy to verify sensibilization with the pre-dose. Fig. 4(a) shows the normalized intensity (with the intensity of the pellet without pre-dose) as a function of the pre-dose. This result shows that the maximum sensitization of the pellets (on the order of 110

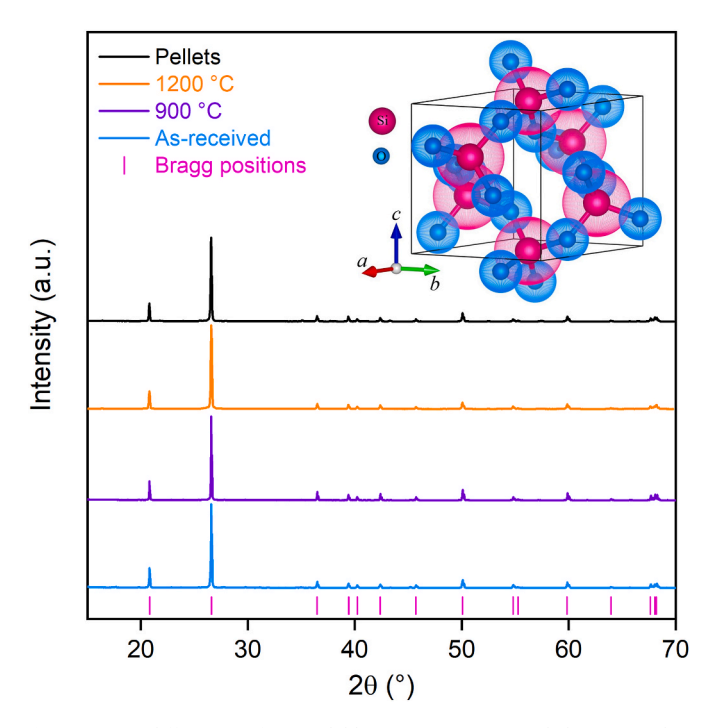


Fig. 3. X-ray diffraction of natural blue quartz as received, heat-treated at 900 $^{\circ}$ C, 1200 $^{\circ}$ C, and sensitized pellets. The vertical lines (pink color) indicate the Bragg positions of the quartz pattern (JCPDS 05–0492). In the inset of the figure, the unit cell structure of the quartz is designed with the VESTA program. (For interpretation of the references to color in this figure legend, the reader is referred to the Web version of this article.)

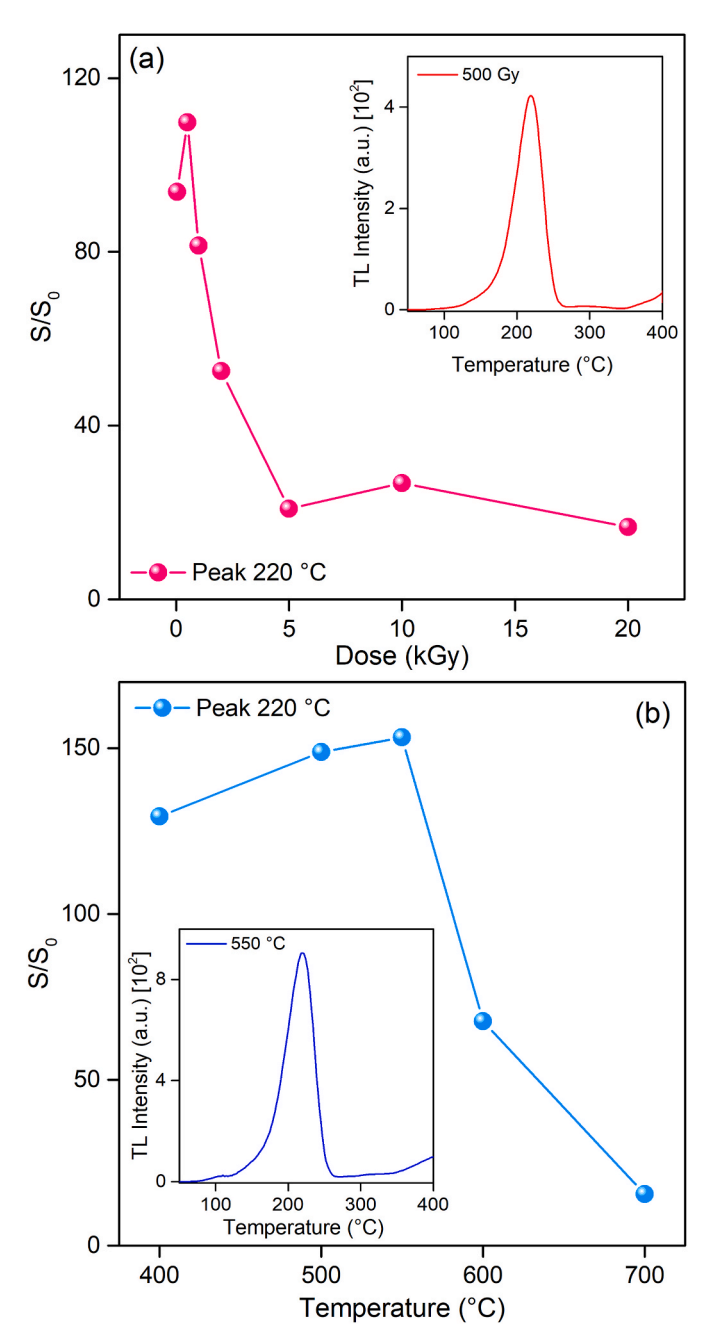


Fig. 4. (a) Behavior of the S/S_0 sensitization curve as a function of the predoses applied to the pellets. The inset of the figure shows the TL glow curve for a sensitization dose of 500 Gy using a test dose of 1 Gy. (b) S/S_0 sensitization response of the pellets as a function of activation temperatures. The inset of the figure shows the TL glow curve for an activation temperature of 550 °C and a test dose of 1 Gy.

times) occurs for a pre-dose of 500 Gy. The inset of Fig. 4(a) shows the TL glow curve of blue quartz pellets sensitized with a pre-dose of 500 Gy.

Blue quartz pellets sensitized with a pre-dose of 500 Gy were divided into five groups and subjected to different thermal activation temperatures: 400, 500, 550, 600, and 700 °C. Fig. 4(b) shows the intensity of the TL peak at 220 °C as a function of thermal activation temperature. This result evidences a maximum increase of its TL response by 150 times for a thermal activation temperature of 550 °C. The inset of Fig. 4 (b) shows the TL glow curve obtained for the thermal activation temperature at 550 °C.

From these results, sensitized pellets were obtained for further studies using the following procedure: pellet sintering temperature 1200 $^{\circ}\text{C},$ irradiation of 500 Gy, and thermal activation temperature 550 $^{\circ}\text{C}.$

The 3D (bottom) and contour (top) plots of the TL emission from the sensitized blue quartz pellets are shown in Fig. 5. It can be seen that the main peak at 220 $^{\circ}$ C shows an emission band centered at 370 nm. A lower intensity TL emission band is also observed at 455 nm that contributes to the TL emission peak around 430 $^{\circ}$ C.

For the analysis of the kinetic parameters of the individual peaks composing the TL glow curve of the sensitized blue quartz pellet, the methods of vary heating rates (VHR) [24], Tm-Tstop [25], and deconvolution [19] were used.

Using the variable heating rate method, the sensitized blue quartz pellets were initially irradiated with a gamma dose of 1 Gy, after which the TL glow curve was recorded at different heating rates ranging from 1 to 8 °C/s. As shown in Fig. 6(a), the main TL peak shifts to higher temperatures, from 203 °C to 245 °C, while the TL intensity decreases with increasing heating rate, with the area under the peak curve decreasing as the heating cycle progresses (see the inset in Fig. 6(a)), indicating that the material is undergoing thermal quenching. Consequently, the activation energy obtained by this method Fig. 6(b) is 0.99 (9) eV. The linear fit, with a correlation coefficient of $\rm r^2=0.98$, suggests that the effect of the lag to exist remains within the acceptable uncertainty margins of the experimental methods.

The results of the Tm-Tstop method, shown in Fig. 7, are compatible with at least three components: the first one linked with localized electron trap distributions, while the second and third ones also correspond to continuous trap distributions. Furthermore, in the results of the linearity analysis of the TL response with absorbed dose, no shift of the TL glow curve toward higher temperatures was observed with increasing absorbed dose. This behavior is consistent with the models associated with first-order kinetics.

Finally, based on the results of the above analysis, the kinetic parameters of each individual peak in the TL glow curve have been estimated using deconvolution fitting (CGCD) [19].

Fig. 8 shows the similarity between the experimental and theoretical glow curve obtained by deconvolution by the CGCD method for samples

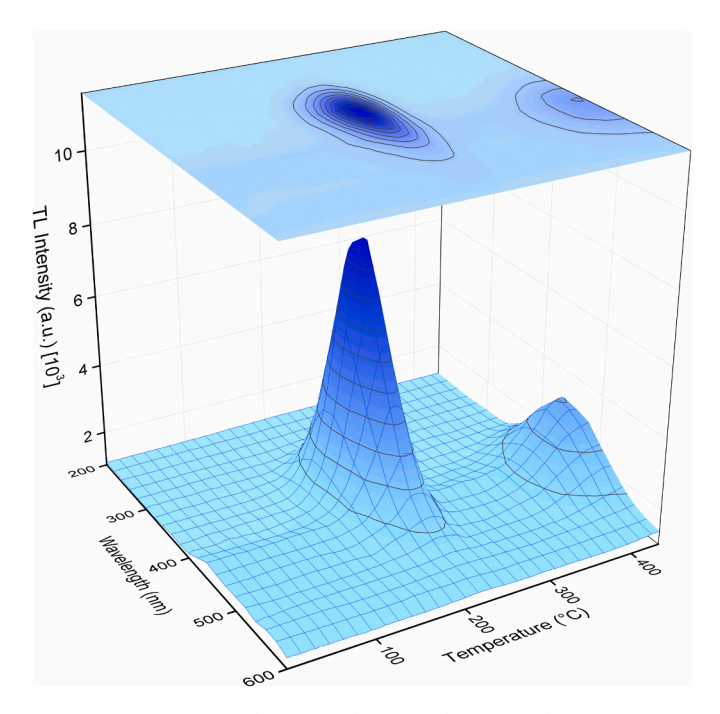


Fig. 5. 3D representation (bottom) and contour plot (top) of the TL spectrum of blue quartz sample irradiated with a dose of 5 Gy. (For interpretation of the references to color in this figure legend, the reader is referred to the Web version of this article.)

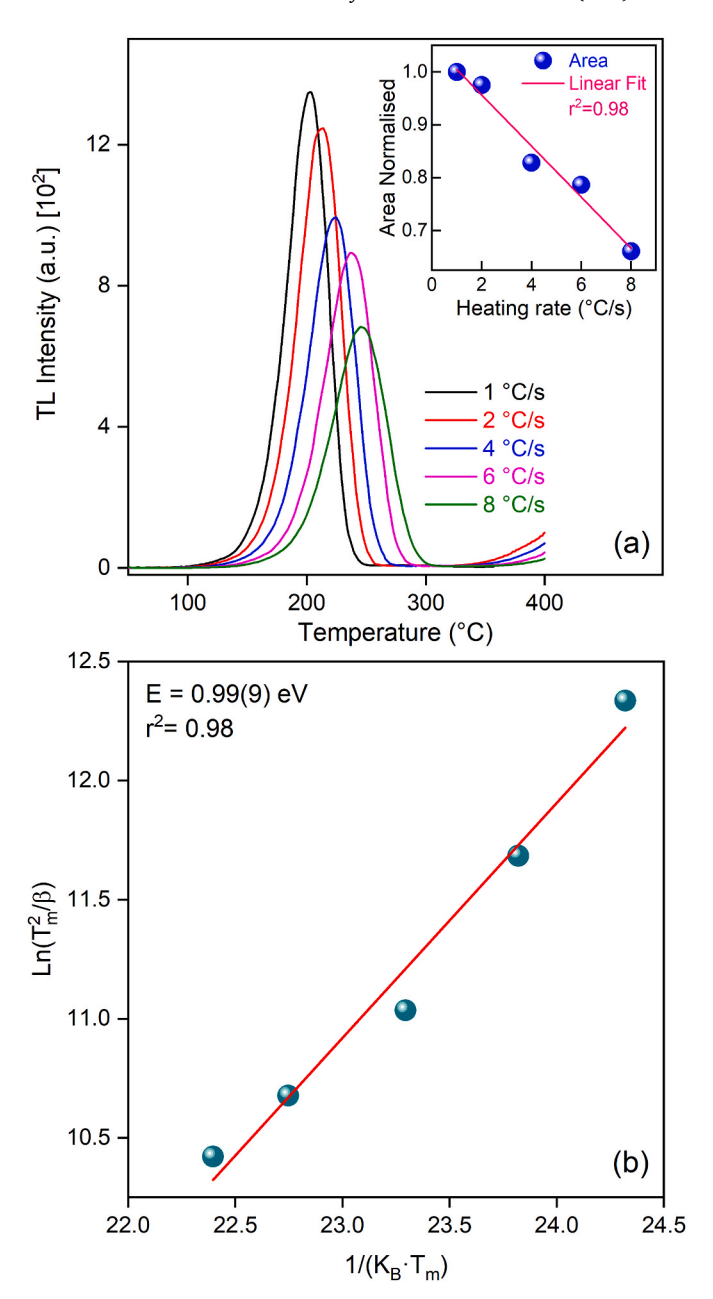


Fig. 6. (a) TL glow curves for the blue quartz pellet read at different heating rates. In the inset of the figure, the position of the peak as a function of heating rate. (b) Plot of $Ln(T_m^2/\beta)$ versus $1/K_\beta Tm$ to evaluate activation energy with variable heating rate method. (For interpretation of the references to color in this figure legend, the reader is referred to the Web version of this article.)

irradiated with gamma doses between 0.3 and 10 Gy. A figure of merit (FOM) [26] lower than 2.79% shows a good fit between the experimental results and those calculated by CGCD. The peak positions and trap parameters are shown in Table 2. The deconvolution analysis results show an 18 % higher value for the second contribution compared to those obtained using the VHR method. This difference arises from the alteration caused by the thermal quenching phenomenon in the VHR method.

3.3. Dosimetric properties analysis

For the dosimetric properties analysis, 95 pellets (sintered at $1200\,^{\circ}$ C) sensitized with a pre-dose of 500 Gy and a thermal activation temperature of 550 $^{\circ}$ C were produced. Not all pellets in this group

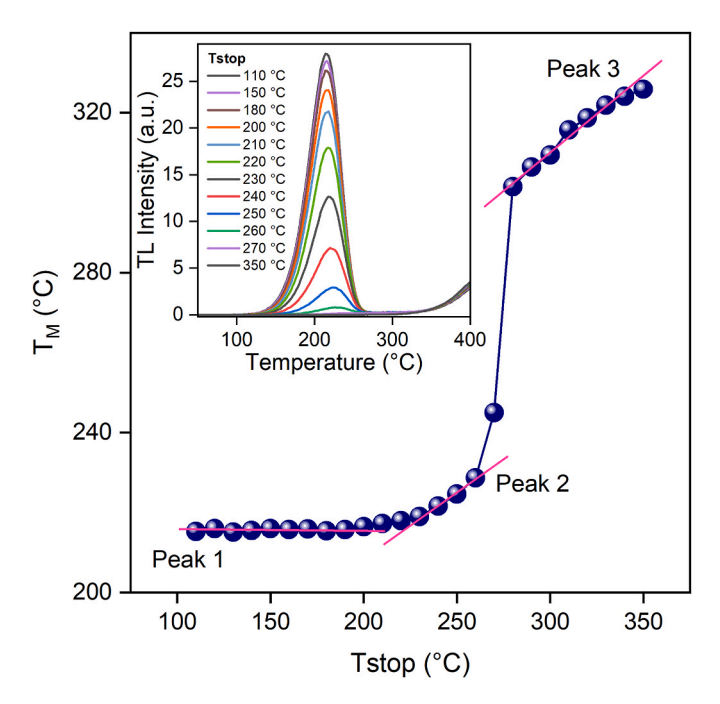


Fig. 7. Tm-Tstop behavior: Maximum intensity (Tm) as a function of the heat treatment temperature prior to the TL reading (Tstop). The inset figure shows some TL glow curves for different Tstop.

showed the same TL intensity for the 220 $^{\circ}$ C peak. Due to this behavior, we proceeded to select the pellets using the detector variability index. To select the blue quartz pellets, five TL readout cycles were performed: heat treatment at 400 $^{\circ}$ C, irradiation with a test dose of 1 Gy, and TL readout. To select the pellets, we used the following exclusion criteria: (a) individual dispersion of the TL intensity greater than 10 %; (b) mean value of the TL intensities outside the 1 sigma interval. The evaluation of the heterogeneity of the batch of produced pellets was estimated by the detector variability index (DVI) [27], which allows for measuring the reproducibility of the batch of produced blue quartz pellets, giving a value of DVI equal to 3.0%.

3.3.1. Linearity

For dosimetric application purposes, the relationship between TL intensity and absorbed dose should be directly proportional. Fig. 9(a) and (b) show the behavior of peak TL intensity at 220 $^{\circ}\text{C}$ as a function of dose between 0.3 and 50 Gy for the sample irradiated with a ^{60}Co (1250 keV) source and for doses between 5 and 60 mGy irradiated with a ^{137}Cs (665 keV) source, respectively.

To evaluate the linearity of the TL intensity behavior as a function of the dose of the blue quartz pellets, we determined the supralinearity index [28] defined by the following equation:

$$F(D) = \frac{S_D}{S_{D_1}} \tag{7}$$

where S_D is the TL intensity of the peak at 220 °C for dose D and D_1 is the lowest dose in the linear dose interval. When F(D)=1, it indicates the linearity interval; for F(D)>1, it indicates the supralinearity interval; and for F(D)<1, it indicates the sublinearity interval. At the bottom of Fig. 9(a) and (b) are presented as the plot of the supralinearity index for both dose regions analyzed in this work (blue balls). For the blue quartz pellets irradiated with a 60 Co source, they present a linearity behavior for the 0.3 and 8 Gy region, and for doses above this value, the pellets present a sublinearity behavior. On the other hand, for the pellets irradiated with a 137 Cs source, they present a linearity behavior for the 5–40 mGy dose region.

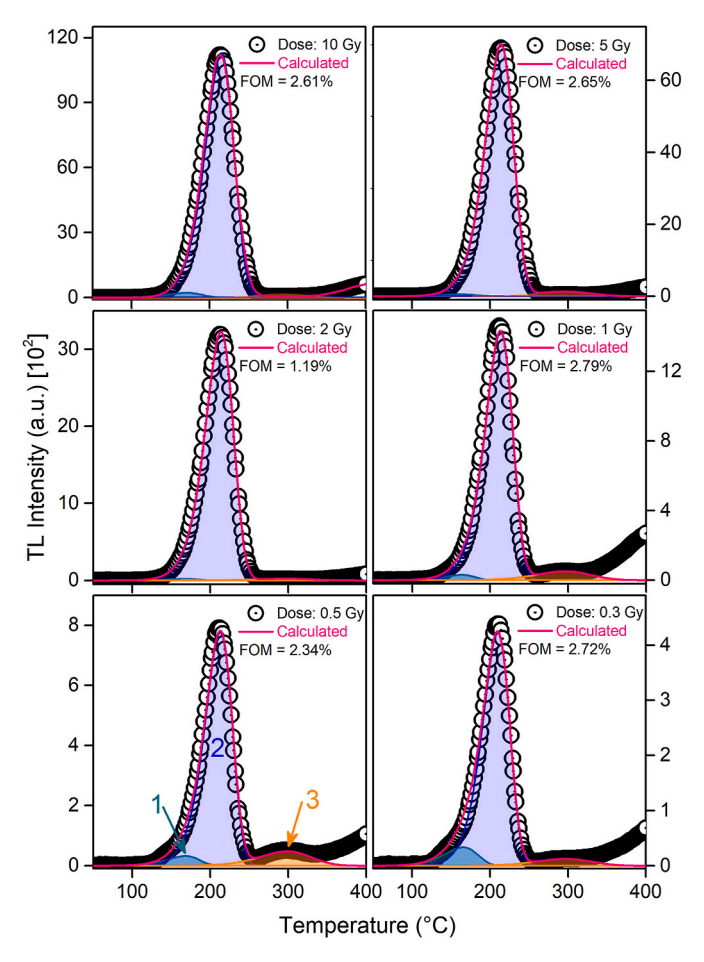


Fig. 8. Glow curve deconvolution graph for blue quartz pellets irradiated with gamma doses of 0.3, 0.5, 1, 2, 5, and 10 Gy. (For interpretation of the references to color in this figure legend, the reader is referred to the Web version of this article.)

Table 2 Kinetic parameters of TL peaks of blue quartz pellets obtained by deconvolution method: maximum temperature (T_M) , activation energy (E), distribution width (σ) , and frequency factor (s).

Peak	T _M (°C)	E (eV)	σ (eV)	s (s ⁻¹)
1	167(1)	0.79(1)	0.0	4(1)·10 ⁸
2	214(1)	1.204(1)	0.0161(5)	$7(1)\cdot 10^{11}$
3	300(1)	0.937(9)	0.033(1)	$2.5(4)\cdot10^{7}$

3.3.2. Fading of TL signal

TL dosimeters (TLD) should be able to store the absorbed dose until they are stimulated for reading. However, some dosimetric materials may emit photons spontaneously, which causes loss of the TL signal before measurement and thus may result in an underestimation of the absorbed dose. To ensure the accuracy of a dosimeter, the loss during fading should be less than 5% [29].

To evaluate the fading of the TL signal peak at around 220 $^{\circ}$ C, 10 groups of blue quartz pellets (each group of 5 pellets) were irradiated with a dose of 1 Gy and stored in a dark place at room temperature. The reading of the first group of pellets was taken 2 h after irradiation; that of the second group, 4 h later, and so on until that of the last group, which corresponds to 1440 h of storage (approximately 60 days). The result of the peak intensity fading at 220 $^{\circ}$ C is shown in Fig. 10. It is observed that the intensity decreases by 3.2% in the first 12 h and that, for times longer than this value, there are no significant variations in its intensity.

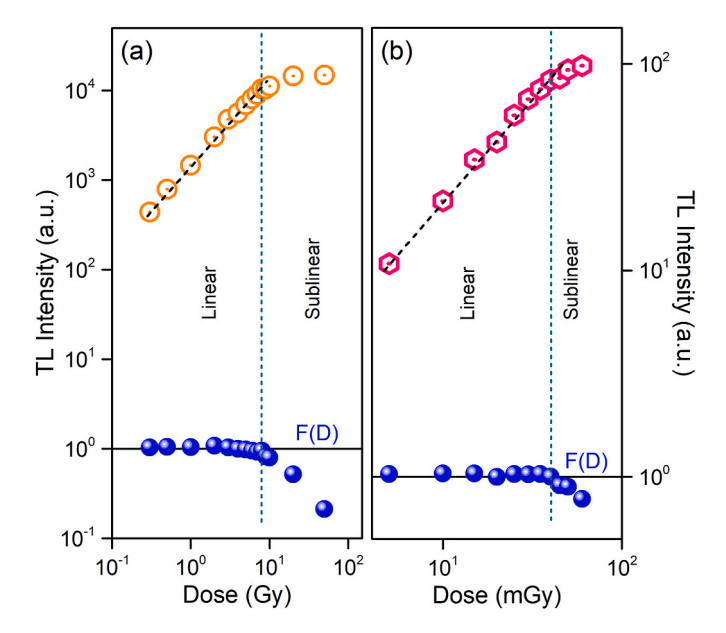


Fig. 9. TL intensity behavior as a function of gamma radiation dose (top) and the linearity index for peak 220 $^{\circ}$ C (bottom), the black line represents the linearity index.

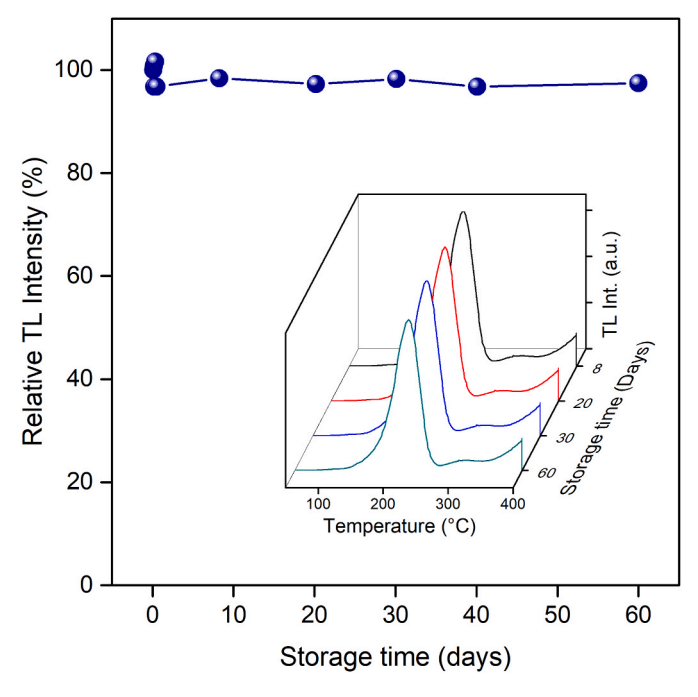


Fig. 10. Fading of TL intensity with storage time. The inset of the figure shows the TL glow curves of the blue quartz pellets after different storage times. (For interpretation of the references to color in this figure legend, the reader is referred to the Web version of this article.)

3.3.3. Reproducibility and repeatability

The reproducibility and repeatability of the TL signal of the blue quartz pellets are necessary to ensure the degree of confidence in the overall results during their application in TL dosimetry. To study reproducibility, a batch of 10 pellets was prepared and irradiated with a dose of 1 Gy and then the TL signal of each pellet was recorded. On the other hand, to study repeatability, one of these pellets was subjected to several cycles of annealing-irradiation-reading. Each cycle consisted of the following: (i) annealing at 400 $^{\circ}\mathrm{C}$ for 30 min, (ii) irradiation with a dose of 1 Gy, and (iii) TL reading in the temperature range from 50 to

400 °C. The degree of reproducibility and repeatability was performed by analyzing the coefficient of variation (C.V.), which must have a value of less than 5% for a dosimeter to be reproducible/repeatable [30]. The results of the reproducibility and repeatability analysis are shown in Fig. 11(a) and (b), respectively, with a C.V. of 1.2% for reproducibility and 1.17% for repeatability.

3.3.4. Sensitivity

The sensitivity of a dosimeter is determined by comparing the TL intensity of the sample under investigation with that of a standard dosimeter, the dosimeter with the highest sensitivity being the one with the highest TL intensity [25]. For this purpose, two materials are irradiated with the same dose under the same irradiation conditions, and TL readings are taken under the same conditions. To evaluate the sensitivity of blue quartz pellets, commercial TLD-100 dosimeters have been used. For this purpose, quartz pellets and the TLD-100 dosimeter were irradiated with the same gamma irradiation dose of 1 Gy. For comparison purposes, the intensity of both materials was normalized to mass. Fig. 12 shows that the sensitivity of the blue quartz is half that of the commercial TLD-100 dosimeter.

3.3.5. Minimum detectable dose (MDD)

The minimum detectable dose (MDD) is the lowest dose that can be measured by a dosimeter using a given TL measurement equipment, so its value is very close to the noise or background signal region of the TL reader. The determination of the MDD value of a given dosimeter allows, in particular, to establish the detection limit for a given dosimetric application. In this work, the DDM value was determined using the empirical equation proposed by Furetta et al. [31].

$$MDD = (B + 2\sigma_B) \bullet F(xx)$$
 (8)

where B is the mean value of the background TL readings, σ_B is the standard deviation of the background TL readings, and F is the calibration factor of the detection system.

The blue quartz pellets were exposed to a dose of 1 Gy, and the TL signal was recorded as the first reading. Then, the background TL signal was recorded 10 times sequentially. The mean value of the background

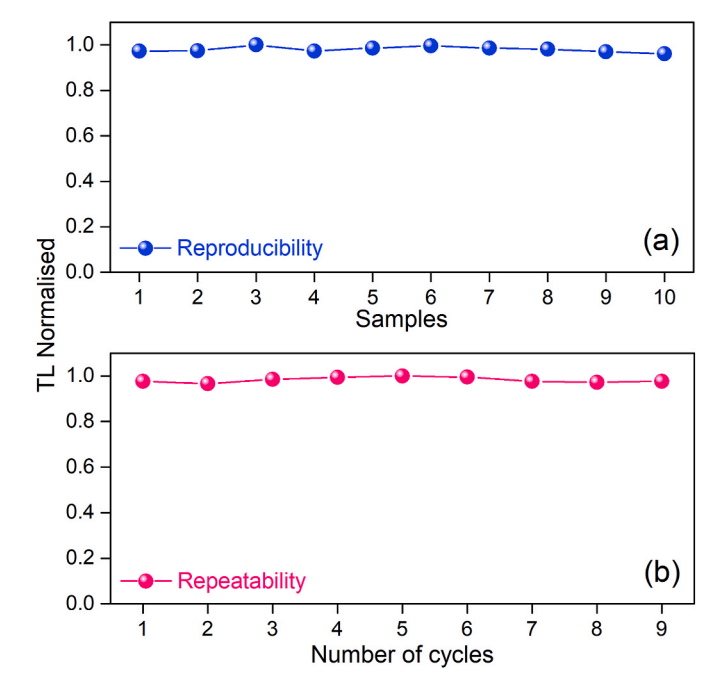


Fig. 11. (a) Reproducibility from 10 pellets with the same mass irradiated with 1 Gy gamma rays. (b) Repeatability from 10 TL readout cycles using the same conditions (dose = 1 Gy).

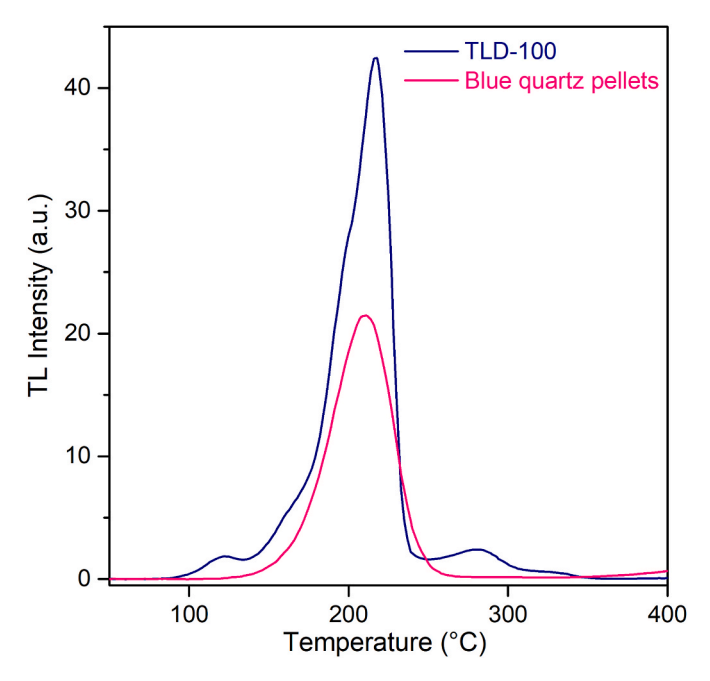


Fig. 12. Comparison of the normalized TL glow curves with their respective mass (dose =1 Gy).

TL readings (*B*) was 0.10083, the standard deviation of these background TL signals σ_B was found to be 0.03424 and the calibration factor (*F*) was 1.37×10^{-5} . All these values were substituted into equation (8) to determine the MDD value, resulting in $2.32 \mu Gy$.

3.3.6. Energy dependence

For dosimetry applications, the dosimetric material irradiated with the same dose shouldn't present variations in its TL response when irradiated with sources of different energies; that is, it does not present an energy dependence [32].

Fig. 13(a) shows the behavior of the peak TL intensity at 220 °C as a function of doses for the four different irradiation sources. It is observed that, in general, the response is linear over the analyzed dose range. Fig. 13(b) shows the energy dependence for the energy range between 34 keV and 1250 keV, where it is observed that the blue quartz pellets present an energy dependence for low energies, predominating for this region the photoelectric effect. The inset of Fig. 13(b) shows the TL glow curves of blue quartz pellets irradiated with sources of different energies: X-rays, with an energy of 34 keV; X-rays, with an energy of 64 keV; gamma rays from a ¹³⁷Cs source with an energy of 662 keV; and gamma rays from a ⁶⁰Co source with an energy of 1250 keV. We can observe that the shape of the TL glow curve and the position of the TL peak are similar and remain in the same position for all four types of energy, except for the TL intensity, which varies as a function of energy.

4. Conclusions

The results of XRF, XRD, SEM, and EDS analysis indicate that the chemical composition and structure, respectively, correspond to crystalline quartz with trigonal structure. The impurities present in natural blue quartz in higher concentrations are Al and K, and in lower concentrations, Fe, Ti, P, Ca, Zr, and Sr. The best sensitization of sintered blue quartz pellets at 1200 °C was obtained by a pre-dose of 500 Gy, followed by a thermal activation temperature of 550 °C. The TL glow curve of the blue quartz pellet calculated by Tm-Tstop and deconvolution methods shows three TL peaks centered at 167, 214, and 300 °C, with activation energies of 0.79, 1.204, and 0.93 eV, respectively. The blue quartz pellets show linearity in their TL response in the dose range from 0.03 Gy to 8 Gy and between 5 mGy and 40 mGy when irradiated

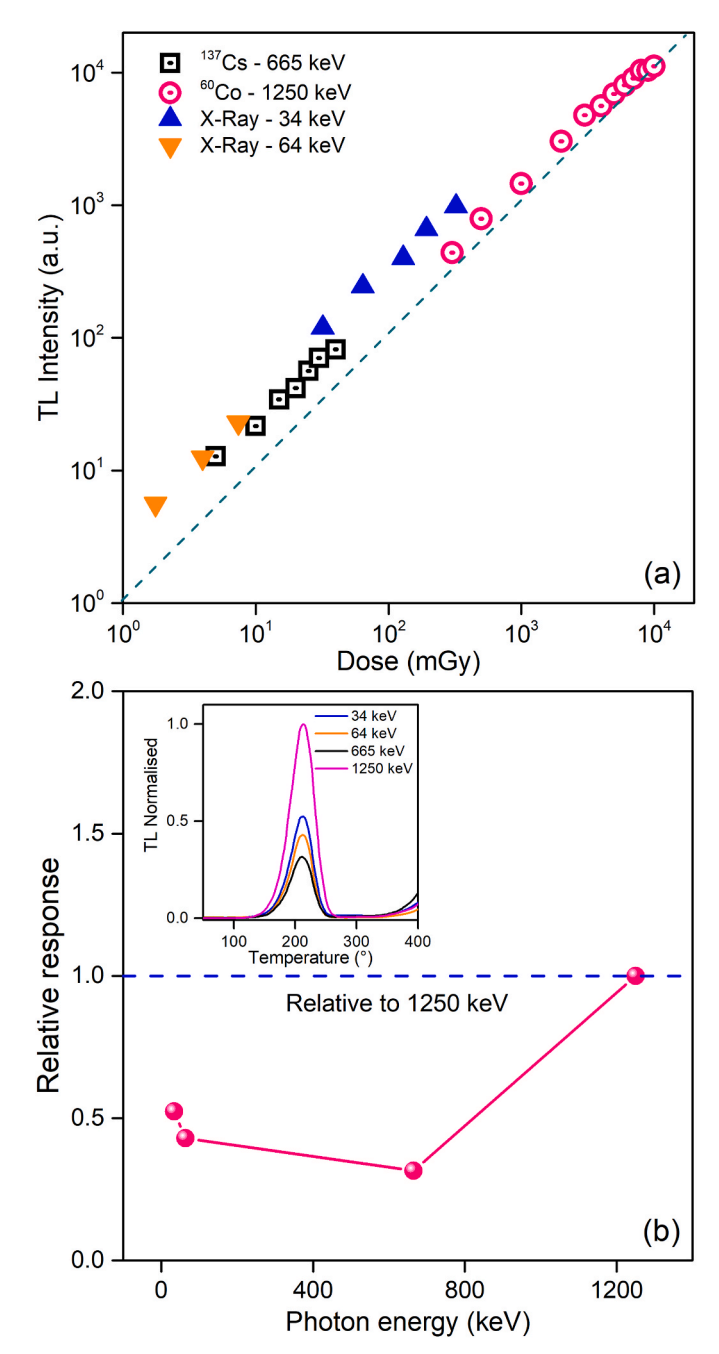


Fig. 13. (a) Behavior of the peak TL intensity at 220 $^{\circ}$ C as a function of the irradiation dose for different sources with different energies. (b) TL intensity response relative to the intensity obtained for 60 Co at an energy of 1250 keV. The inset of the figure, TL glow curves of blue quartz pellets irradiated with different radiation sources, 34 keV and 64 keV X-rays, 665 and 1250 keV, 137 Cs and 60 Co sources, respectively. (For interpretation of the references to color in this figure legend, the reader is referred to the Web version of this article.)

with a 60 Co and 137 Cs source, respectively. The signal fading of the blue quartz pellets is 3.2% in the first 12 h and then shows good stability at room temperature. The TL signal from the blue quartz pellets proved to be reproducible, with a C.V. of 1.20% in 10 samples, and repeatable for the same sample with a C.V. of 1.17%. In addition, the sensitivity of the blue quartz pellets is 0.5 times the TL intensity of the commercial dosimeter TLD-100. Finally, these pellets exhibit energy dependence for low energies, where the photoelectric effect predominates.

CRediT authorship contribution statement

Betzabel N. Silva-Carrera: Writing – original draft, Methodology, Investigation, Formal analysis, Data curation, Conceptualization, Writing – review & editing. Nilo F. Cano: Writing – original draft, Visualization, Validation, Supervision, Software, Methodology, Investigation, Formal analysis, Conceptualization, Writing – review & editing. Felix V.S. Cruz: Investigation, Formal analysis, Data curation. Edwin J. Pilco: Software, Investigation, Formal analysis, Data curation, Methodology. T.K. Gundu Rao: Writing – original draft, Visualization, Validation, Supervision, Methodology, Formal analysis, Data curation, Writing – review & editing. J.F. Benavente: Validation, Software, Methodology, Investigation, Formal analysis, Writing – original draft, Writing – review & editing. José F.D. Chubaci: Validation, Investigation, Funding acquisition, Formal analysis, Conceptualization, Supervision, Visualization.

Declaration of competing interest

The authors declare that they have no known competing financial interests or personal relationships that could have appeared to influence the work reported in this paper.

Acknowledgements

The authors are very grateful to Ms. E. Somessari and Mr. Aldo Oliviera, Instituto de Pesquisas Energéticas e Nucleares (IPEN/CNEN-SP) for kindly carrying out the irradiation of the samples. This work was partially supported by PROCIENCIA-CONCYTEC, Peru, in the framework of the call E041- 2023-01 (Process number PE501082822-2023-PROCIENCIA).

Data availability

Data will be made available on request.

References

- [1] M. Lamothe, A. Dreimanis, M. Morency, A. Raukas, Thermoluminescence dating of quaternary sediments, Dev. Palaeontol. Stratigr. 7 1(984) 153-170. https://doi. org/10.1016/S0920-5446(08)70070-0.
- [2] A.G. Wintle, D.J. Huntley, Thermoluminescence dating of sediments, Quat. Sci. Rev. 1 (1982) 31–53, https://doi.org/10.1016/0277-3791(82)90018-X.
- [3] S.J. Fleming, Thermoluminescent dating: refinement of the quartz inclusion method, Archaeometry 12 (1970) 133–143, https://doi.org/10.1111/j.1475-4754.1970.tb00016.x.
- [4] M.A. Seeley, Thermoluminescent dating in its application to archaeology: a review, J. Archaeol. Sci. 2 (1975) 17–43, https://doi.org/10.1016/0305-4403(75)90044-8
- [5] I.K. Bailiff, L. Bøtter-Jensen, V. Correcher, A. Delgado, H.Y. Göksu, H. Jungner, S. A. Petrov, Absorbed dose evaluations in retrospective dosimetry: methodological developments using quartz, Radiat. Meas. 32 (2000) 609–613, https://doi.org/10.1016/S1350-4487(00)00076-7.
- [6] F. Preusser, M.L. Chithambo, T. Götte, M. Martini, K. Ramseyer, E.J. Sendezera, G. J. Susino, A.G. Wintle, Quartz as a natural luminescence dosimeter, Earth Sci. Rev. 97 (2009) 184–214, https://doi.org/10.1016/j.earscirev.2009.09.006.
- [7] A.D. Franklin, J.R. Prescott, R.B. Scholefield, The mechanism of thermoluminescence in an Australian sedimentary quartz, J. Lumin. 63 (1995) 317–326, https://doi.org/10.1016/0022-2313(94)00068-N.
- [8] T.M.B. Farias, S. Watanabe, A comparative study of the thermoluminescence properties of several varieties of Brazilian natural quartz, J. Lumin. 132 (2012) 2684–2692, https://doi.org/10.1016/j.jlumin.2012.04.047.
- [9] C.A. Márquez-Mata, H.R. Vega-Carrillo, M.J. Mata-Chávez, M.G. Garcia-Reyna, J. Vazquez-Bañuelos, G.E. Campillo-Rivera, Á. García-Duran, C.O. Torres-Cortes, I. Rosales-Candelas, J.J. Soto-Bernal, Thermoluminescent characteristics of seven

- varieties of quartz, Mater. Chem. Phys. 295 (2023) 126999, https://doi.org/10.1016/j.matchemphys.2022.126999.
- [10] J. Zimmerman, The radiation-induced increase of the 100 C thermoluminescence sensitivity of fired quartz, J. Phys. C Solid State 4 (1971) 3265, https://doi.org/ 10.1088/0022-3719/4/18/032.
- [11] R.B. Scholefield, J.R. Prescott, A.D. Franklin, P.J. Fox, Observations on some thermoluminescence emission centres in geological quartz, Radiat. Meas. 23 (1994) 409–412, https://doi.org/10.1016/1350-4487(94)90072-8.
- [12] N. Itoh, D. Stoneham, A.M. Stoneham, Ionic and electronic processes in quartz: mechanisms of thermoluminescence and optically stimulated luminescence, J. Appl. Phys. 92 (2002) 5036–5044, https://doi.org/10.1063/1.1510951.
- [13] W.J. Rink, H. Rendell, E.A. Marseglia, B.J. Luff, P.D. Townsend, Thermoluminescence spectra of igneous quartz and hydrothermal vein quartz, Phys. Chem. Miner. 20 (1993) 353–361, https://doi.org/10.1007/BF00215106.
- [14] H.J. Khoury, P.L. Guzzo, S.B. Brito, C.A. Hazin, Effect of high gamma doses on the sensitization of natural quartz used for thermoluminescence dosimetry, Radiat. Eff. Defect Solid 162 (2007) 101–107, https://doi.org/10.1080/10420150601035490.
- [15] P.L. Guzzo, H.J. Khoury, M.R. Miranda, S.B. Barreto, A.H. Shinohara, Point defects and pre-dose requirements for sensitization of the 300°C TL peak in natural quartz, Phys. Chem. Mineral. 36 (2009) 75–85, https://doi.org/10.1007/s00269-008-0050 y
- [16] S.R. Nascimento, L.B. Souza, H.J. Khoury, P.L. Guzzo, Study of dosimetric properties of sensitized Solonópole quartz. International Nuclear Atlantic Conference - INAC, 2009.
- [17] Á.B.C. Junior, T.F. Barros, P.L. Guzzo, H.J. Khoury, Manufacturing polycrystalline pellets of natural quartz for applications in thermoluminescence dosimetry, Mater. Res. 15 (2012) 536–543, https://doi.org/10.1590/S1516-14392012005000075.
- [18] J.U.G.F. Cunha, Á.B.C. Júnior, R.R. Rocca, L.B.L. Souza, A.S.M. Lacerda, M.H. T. Lopes, N.F.S. Neto, Propriedades dosimétricas de discos de quartzo expostos a um feixe de raios X para mamografia, Peer Rev. 5 (2023) 48–62.
- [19] J.F. Benavente, J.M. Gómez-Ros, A.M. Romero, Thermoluminescence glow curve deconvolution for discrete and continuous trap distributions, Appl. Radiat. Isot. 153 (2019), https://doi.org/10.1016/j.apradiso.2019.108843.
- [20] S.W.S. McKeever, Thermoluminescence in Solids, Cambridge University Press, Cambridge, 1985.
- [21] J.F. Benavente, O. Arquero, J. Berenguer-Antequera, Effects of trapped charge transitions between localized levels on the optical properties of thermoluminescent materials: a study of fading and thermal quenching, Opt. Mater. 156 (2024) 116006, https://doi.org/10.1016/j.optmat.2024.116006.
- [22] E.O. Oniya, G.S. Polymeris, N.N. Jibiri, N.C. Tsirliganis, I.A. Babalola, G. Kitis, Contributions of pre-exposure dose and thermal activation in pre-dose sensitizations of unfired and annealed quartz, Radiat. Phys. Chem. 110 (2015) 105–113, https://doi.org/10.1016/j.radphyschem.2015.01.033.
- [23] E. Almogait, A.H. Almuqrin, N. Alhammad, M.I., thermoluminescence sensitization of phyllite natural rock, Appl. Sci. 12 (2022) 637, https://doi.org/10.3390/ appl.2020637.
- [24] R. Chen, J.L. Lawless, V. Pagonis, On the various-heating-rates method for evaluating the activation energies of thermoluminescence peaks, Radiat. Meas. 150 (2022) 106692, https://doi.org/10.1016/j.radmeas.2021.106692.
- [25] S.W.S. McKeever, Thermoluminescence in Solids, Cambridge University Press, Cambridge, 1985.
- [26] H.G. Balian, N.W. Eddy, Figure-of-merit (FOM), an improved criterion over the normalized chi-squared test for assessing goodness-of-fit of gamma-ray spectral peaks, Nucl. Instrum. Methods 145 (1977) 389–395, https://doi.org/10.1016/ 0029-554X(77)90437-2
- [27] A.O. Elsheikh, A.A. El-Hafez, M. Moustafa Ahmed, Y.A.A. Abdul-Razek, M.E. El-Nagdy, Quantification of various factors influencing repeatability and reproducibility of TLD-600 detector, Arab J. Nucl. Sci. Appl. 53 (2020) 58–66, https://doi.org/10.21608/ajnsa.2019.13313.1219.
- [28] R. Chen, S.W.S. McKeever, Characterization of nonlinearities in the dose dependence of thermoluminescence, Radiat. Meas. 23 (1994) 667–673, https://doi.org/10.1016/1350-4487(94)90002-7.
- [29] R. Chen, P.L. Leung, M.J. Stokes, Apparent anomalous fading of thermoluminescence associated with competition with radiationless transitions, Radiat. Meas. 32 (2000) 505–511, https://doi.org/10.1016/S1350-4487(00) 00082-2.
- [30] C. Furetta, Handbook of Thermoluminescence, World Scientific Publishing Co. Pte. Ltd, 2003, https://doi.org/10.1142/5167.
- [31] C. Furetta, M. Prokic, R. Salamon, V.Prokic G. Kitis, Dosimetric characteristics of tissue equivalent thermoluminescent solid TL detectors based on lithium borate, Nucl. Instrum. Meth. A 456 (2001) 411–417, https://doi.org/10.1016/S0168-9002 (00)00585-4
- [32] V. Ramprasath Shivaramu, Effective atomic numbers for photon energy absorption and energy dependence of some thermoluminescent dosimetric compounds, Nucl. Instrum. Meth. B 168 (2000) 294–304, https://doi.org/10.1016/S0168-583X(99) 01100-3